

Differential quadrature method for space-fractional diffusion equations on 2D irregular domains

X. G. Zhu · Y. F. Nie · Z. B. Yuan

Received: date / Accepted: date

Abstract In mathematical physics, the space-fractional diffusion equation is of practical interest in the studies of physical phenomena modelled by the Lévy processes, which is sometimes called super-diffusion equation. In this article, we propose new differential quadrature (DQ) methods for solving the 2D space-fractional diffusion equations with fractional directional derivatives. The methods in presence directly convert the original problem into a set of ordinary differential equations (ODEs) via approximating the fractional derivatives as weighted linear combinations of the functional values at scattered points on the whole domain. The required weighted coefficients are calculated by using radial basis functions (RBFs) as test functions and the resultant ODEs are discretized by the Crank-Nicolson scheme. The main advantages of our methods lie in their flexibility and the applicability to 2D irregular domains. A series of illustrated examples are finally provided to confirm these points.

Keywords DQ method · radial basis functions (RBFs) · fractional directional derivatives · space-fractional diffusion equations · irregular domains

Mathematics Subject Classification (2010) 35R11 · 65D25 · 65M99

1 Introduction

During recent decades, a bulk of attention has been attracted to a special part of partial differential equations (PDEs), i.e., the so-called fractional PDEs,

X. G. Zhu · Y. F. Nie · Z. B. Yuan

Department of Applied Mathematics, Northwestern Polytechnical University, Xi'an, Shaanxi 710129, P. R. China

E-mail: yfnie@nwpu.edu.cn

X. G. Zhu

E-mail: zhuxg590@yeah.net

Z. B. Yuan

E-mail: yzzzb@nwpu.edu.cn

especially those abstracted from practical problems. As a class of new mathematical models, fractional PDEs show good promise in characterizing the memory effort and historical dependence of the physical processes like the anomalous dispersion in complex heterogeneous aquifer and the medium with fractal geometry [1, 29], thereby making up the deficiency of inconsistency with the reality when an integer-order model is utilized to describe the similar non-classical phenomena. The relevant applications include crystal dislocation, hydrodynamics, electrochemistry, plasma turbulence, continuum mechanics, and so forth [8, 20, 25, 28, 32]. There is still a rapidly growing interest on such subjects in this moment. Due to the universal mutuality, however, their solutions can rarely be represented by elementary functions in closed forms. A few existent analytic solutions are limited to very simple cases or achieved in series or integral forms under theoretical restrictions; see [30, 35, 36, 49] and references therein. This presents a severe challenge for developing sufficiently valid analytic techniques for these equations, so numerical algorithms has been favored and gradually emerged as essential alternatives in actual investigation.

The space-fractional PDEs constitute an important branch of PDEs in studies on the evolution of probability density distribution of the diffusion particle state. As compared to the time-fractional PDEs, seeking the approximate solutions to such equations appears to be more difficult by virtue of the highly complex fractional Laplacian. Up to date, various numerical algorithms have been designed, covering finite difference methods [18, 26, 27, 39, 44, 45], general Padé approximation [12], meshless point interpolation method [23, 50], finite element methods [11, 16], discontinuous Galerkin method (DGM) [47], finite volume methods [19, 21], spline approximation method (SAM) [43], and spectral collocation methods [5, 2, 51]. In [9, 13, 37, 40], a series of operational matrix methods are constructed based on the approximate expansions by using shifted Jacobi, Chebyshev, Legendre polynomials, and Haar wavelets functions, as elements, respectively. In [52], a Crank–Nicolson alternating direction implicit Legendre–Galerkin spectral method has been derived for the 2D Riesz space-fractional nonlinear reaction-diffusion equations. Du and Wang developed a finite element method (FEM) conjectured with a fast algebraic solver for the stationary space-fractional diffusion equations by dividing the unit square domain into structured meshes [14]. It is noteworthy that, nevertheless, all of above mentioned algorithms are only available for the one-dimensional or rectangular domain problems. Few works goes for a valid method for fractional problems on irregular domains. Liu et. al solved a 2D fractional FitzHugh–Nagumo monodomain model by an implicit semi-alternating direction difference method on a specific irregular domain with rectangular mesh [22], where the nodal points need to be artificially assigned to match the boundary. In [53], we proposed a fully discrete FEM for space-fractional Fisher’s equation on regular domains and the generated meshes are relaxed to be unstructured; later, it has been extended to the space-fractional diffusion equations solved on polygonal and elliptic domains [48]. Deng et. al developed a nodal DGM for the same type equations on unstructured triangular meshes and a L-shaped domain problem has been considered [33]. In general, finite difference method

(FDM) is implemented on pre-defined meshes and inherits the shortcomings including the difficulty in simulation of complex domain problems. DGM and FEM alleviate this issue, but both of them hinge on variational principles and suffer expensive computing burden and inflexibility to calculate the entities of their stiffness matrices that are on longer sparse because of the non-local properties of fractional derivatives.

DQ method is understood as a direct numerical approach for finding the solutions of PDEs by reducing the equations into ODEs via approximating the space derivatives as the weighted linear sums of the functional values at finite nodal points on problem domains. It was pioneered by Bellman and Casti [3], and further studied based on different basis functions, such as Lagrangian interpolation basis functions, RBFs, orthogonal polynomials, sinc and spline basis functions [4, 6, 34, 42, 46]. DQ method can achieve high accuracy by using only a few nodal points; besides, it is straight forward to implement and truly meshless. In this context, regarding the current interest in fractional PDEs as effective models, we attempt to establish new DQ methods to solve the space-fractional diffusion equations on 2D irregular domains. The Multi-quadric, Inverse Multiquadric, and Gaussian RBFs are chosen as test functions to determine the weighted coefficients that we require to evaluate the 2D fractional directional derivatives as the representative weighted linear sums of the functional values at scattered or regularly distributed points on the whole domain; a Crank-Nicolson scheme is employed to advance the solutions in time. The proposed methods extend the capabilities of traditional DQ methods and meanwhile inherits their principal merits. A series of illustrated tests are carried out to demonstrate their performance in actual computation, including the square, trapezoidal, and circular domain problems.

The skeleton is organized as follows. In Section 2, the space-fractional diffusion equations on a 2D domain are introduced for preliminaries. Section 3 studies the DQ formulations for fractional directional derivatives and how to determine the weighted coefficients by means of those RBFs. In Section 4, we construct time-stepping DQ methods by using a Crank-Nicolson scheme in time and show the details of implementation. In Section 5, illustrative tests on both regular and irregular domains are preformed to examine their accuracy and effectiveness, and a concise remark is finally drawn in the last section.

2 Model problems

On a given bounded domain $\Omega \subset \mathbb{R}^2$ with its boundary being $\partial\Omega$, the continuous 2D space-fractional diffusion equations are as follows

$$\frac{\partial u(x, y, t)}{\partial t} - \kappa \int_0^{2\pi} \mathcal{D}_\theta^\alpha u(x, y, t) M(d\theta) = f(x, y, t), \quad (x, y, t) \in \Omega \times (0, T], \quad (1)$$

subjected to the initial and boundary conditions

$$u(x, y, 0) = u_0(x, y), \quad (x, y) \in \Omega, \quad (2)$$

$$u(x, y, t) = g(x, y, t), \quad (x, y) \in \partial\Omega \times (0, T], \quad (3)$$

where $1 < \alpha \leq 2$, κ is the non-negative diffusivity parameter, $M(d\theta)$ is a probability measure on the interval $[0, 2\pi)$, and $f(x, y, t)$ is the pre-prescribed source function. In Eq. (1), $\mathcal{D}_\theta^\alpha u(x, y, t)$ stands for the space-fractional directional derivatives defined in Caputo sense, i.e.,

$$\mathcal{D}_\theta^\alpha u(x, y, t) = \mathcal{I}_\theta^{2-\alpha} \mathcal{D}_\theta^2 u(x, y, t), \quad 0 \leq \theta < 2\pi, \quad (4)$$

with the integer-order directional derivatives

$$\mathcal{D}_\theta^m v(x, y) = \left(\cos \theta \frac{\partial}{\partial x} + \sin \theta \frac{\partial}{\partial y} \right)^m v(x, y), \quad m \in \mathbb{Z}^+,$$

and the fractional directional integration

$$\mathcal{I}_\theta^\mu v(x, y) = \frac{1}{\Gamma(\mu)} \int_0^{z(x, y, \theta)} \omega^{\mu-1} v(x - \omega \cos \theta, y - \omega \sin \theta) d\omega,$$

for $\mu > 0$ while $\mathcal{I}_\theta^\mu v(x, y) = v(x, y)$ for $\mu = 0$. $z(x, y, \theta)$ denotes the distance from the nodal point (x, y) to $\partial\Omega$ in the direction $(-\cos \theta, -\sin \theta)$; see Fig. 1. In particular, when θ is taken to be some special values as 0 and π , $\mathcal{D}_\theta^\alpha u(x, y, t)$ recovers the commonly used Caputo derivatives with regard to variable x , i.e.,

$$\mathcal{D}_0^\alpha u(x, y, t) = \frac{1}{\Gamma(2-\alpha)} \int_{\Gamma_1(x, y)}^x \frac{\partial^2 u(\omega, y, t)}{\partial \omega^2} \frac{d\omega}{(x - \omega)^{\alpha-1}}, \quad (5)$$

$$\mathcal{D}_\pi^\alpha u(x, y, t) = \frac{1}{\Gamma(2-\alpha)} \int_x^{\Gamma_2(x, y)} \frac{\partial^2 u(\omega, y, t)}{\partial \omega^2} \frac{d\omega}{(\omega - x)^{\alpha-1}}, \quad (6)$$

and Eqs. (1)-(3) degenerate into the space-fractional diffusion equations in coordinate forms, which have been the topics of intense research, where $\Gamma_1(x, y)$, $\Gamma_2(x, y)$ are the subsets of $\partial\Omega$ in the left and right sides, respectively, and fulfill $\partial\Omega = \Gamma_1(x, y) \cup \Gamma_2(x, y)$; see Fig. 1. It is noticed that the boundary condition (3) need to be consistent with the model problem; for example, if $\theta = 0$, then it must be zero at the boundary points which the integral lines embedded in fractional derivatives start from, i.e., $g(x, y, t) = 0$, for all $(x, y) \in \Gamma_1(x, y)$, whereas if $\theta = \pi$, it must be zero at the boundary points which the integral lines end with, saying $g(x, y, t) = 0$, for all $(x, y) \in \Gamma_2(x, y)$.

In the sequel, without loss of generality, we consider the multi-order 2D space-fractional diffusion equations of discrete version with variable coefficients

$$\frac{\partial u(x, y, t)}{\partial t} - \sum_{l=1}^L \kappa_l(x, y) \mathcal{D}_{\theta_l}^{\alpha_l} u(x, y, t) = f(x, y, t), \quad (x, y, t) \in \Omega \times (0, T], \quad (7)$$

subjected to the same initial and boundary conditions as

$$u(x, y, 0) = u_0(x, y), \quad (x, y) \in \Omega, \quad (8)$$

$$u(x, y, t) = g(x, y, t), \quad (x, y) \in \partial\Omega \times (0, T], \quad (9)$$

where $1 < \alpha_l \leq 2$, $0 \leq \theta_l < 2\pi$, $M \in \mathbb{Z}^+$, $\kappa_l(x, y)$ are the non-negative diffusivity parameters and satisfy $\sum_{l=1}^L \kappa_l(x, y) \neq 0$, and $\mathcal{D}_{\theta_l}^{\alpha_l} u(x, y, t)$ denote a sequence of Caputo directional derivatives of differential orders.

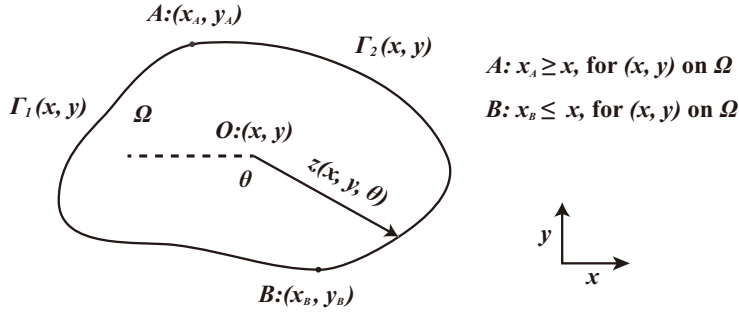


Fig. 1 The subsets of boundary $\Gamma_1(x, y)$, $\Gamma_2(x, y)$, and the distance $z(x, y, \theta)$ of (x, y) .

3 DQ approximations for fractional directional derivatives

In this section, we derive new DQ formulations for approximating the fractional directional derivatives and study how to compute the weighted coefficients by using Multiquadric, Inverse Multiquadric, and Gaussian RBFs as test functions. To start with, let $\Omega \subset \mathbb{R}^2$ be a bounded domain and \mathbf{x}_i , $i = 0, 1, \dots, M$, be a sequence of scattered points distributed on Ω with $\mathbf{x}_i = (x_i, y_i)$. Define a set of proper basis functions $\{\phi_k(\mathbf{x})\}_{k=0}^M$ that are adequately smooth to guarantee the existence of fractional directional derivatives. The essence of DQ method is based on the approximation of partial derivatives of a function with respect to a variable as the weighted linear sums of the functional values at finite discrete points on the overall problem domain. In general, we always approximate the exact solution of a PDE like Eqs. (1)-(3) in the form

$$u(\mathbf{x}, t) \cong \sum_{k=0}^M \delta_k(t) \phi_k(\mathbf{x}), \quad (10)$$

then enforce it to satisfy main equation as well as the related restrictions on collocation points to determine the unknowns $\{\delta_k(t)\}_{k=0}^M$. However, if we have

$$\mathcal{D}_\theta^\alpha \phi_k(\mathbf{x}_i) = \sum_{j=0}^M \omega_{ij}^{(\alpha)} \phi_k(\mathbf{x}_j), \quad i, k = 0, 1, \dots, M, \quad (11)$$

and substitute Eq. (11) into Eq. (10) after acting the differential-integral operator $\mathcal{D}_\theta^\alpha$ on both sides of Eq. (10), it suffices to show that

$$\mathcal{D}_\theta^\alpha u(\mathbf{x}_i, t) \cong \sum_{k=0}^M \delta_k(t) \mathcal{D}_\theta^\alpha \phi_k(\mathbf{x}_i) = \sum_{k=0}^M \delta_k(t) \sum_{j=0}^M \omega_{ij}^{(\alpha)} \phi_k(\mathbf{x}_j) \cong \sum_{j=0}^M \omega_{ij}^{(\alpha)} u(\mathbf{x}_j, t), \quad (12)$$

in the light of the linear property of operator $\mathcal{D}_\theta^\alpha$ — in other words, Eqs. (12) are valid approximations for $\mathcal{D}_\theta^\alpha u(\mathbf{x}_i, t)$, $i = 1, 2, \dots, M$, without knowing $\{\delta_k(t)\}_{k=0}^M$, as long as Eqs. (11) are fulfilled. We term $\omega_{ij}^{(\alpha)}$, $i, j = 0, 1, \dots, M$, by the weighted or DQ coefficients of fractional directional derivatives, which can be computed via Eqs. (11) by formulating them in matrix-vector forms

as priority; $\{\phi_k(\mathbf{x})\}_{k=0}^M$ are referred to as test functions that can typically be chosen by the ones mentioned before. When $\alpha \in \mathbb{Z}^+$ and θ is assigned to be 0, π , Eqs. (12) reduce into the DQ formulations for classical derivatives.

3.1 Radial basis functions

The RBFs are known as a family of spline functions which are constructed from the distance between an arbitrary nodal point \mathbf{x} and its center \mathbf{x}_k , i.e., $\varphi(\|\mathbf{x} - \mathbf{x}_k\|)$, abbreviated to $\varphi_k(\mathbf{x})$, with the Euclidean norm $\|\cdot\|$. These types of functions offer a set of excellent interpolating bases to interpolate the multivariable scattered data on high-dimensional domains and have been served as an efficient tool in setting up truly meshless numerical algorithms for PDEs by virtue of their independency on geometric complexity and the potential spectral accuracy of their interpolations. Among various types of RBFs, three typical kinds of RBFs are concerned hereinafter, i.e.,

- Multiquadric RBFs: $\varphi_k(\mathbf{x}) = \sqrt{\|\mathbf{x} - \mathbf{x}_k\|^2 + \epsilon^2}$,
- Inverse Multiquadrics RBFs: $\varphi_k(\mathbf{x}) = \frac{1}{\sqrt{\|\mathbf{x} - \mathbf{x}_k\|^2 + \epsilon^2}}$,
- Gaussian RBFs: $\varphi_k(\mathbf{x}) = \exp(-\epsilon^2 \|\mathbf{x} - \mathbf{x}_k\|^2)$,

where $k = 0, 1, \dots, M$, $m \in \mathbb{Z}^+$, and ϵ is a user-parameter called by shape number. Given a function $y(\mathbf{x}, t)$ defined on $\Omega \subset \mathbb{R}^d$, $d = 1, 2, 3$, its interpolating approximation based on there trial bases can be written in the form

$$y(\mathbf{x}, t) \cong \sum_{k=0}^M \lambda_k(t) \varphi_k(\mathbf{x}) + \sum_{s=1}^{M'} \lambda_{M+s}(t) p_s(\mathbf{x}), \quad (13)$$

with the unknowns $\{\lambda_k(t)\}_{k=0}^M$, $\{\lambda_{M+s}(t)\}_{s=1}^{M'}$ yet to be determined and subjected to the below additional constraint

$$\sum_{k=0}^M \lambda_k(t) P_{s+1}(\mathbf{x}_k) = 0, \quad M' = \frac{(r+d-1)!}{d!(r-1)!}, \quad (14)$$

to make the generated algebraic system to be well-posed, in which, $\{p_s(\mathbf{x})\}_{s=1}^{M'}$ denote the bases for the polynomial space of degree at most $r-1$ on \mathbb{R}^d . It is worthy to note that the free parameter ϵ should be suitably prescribed in computation because it has a significant impact on the approximate power of the radial basis interpolation, so is a RBFs-based method.

3.2 Determination of weighted coefficients

Before proceeding, we remark that the polynomials in the right side of Eq. (13) is not always necessary since the augmented interpolation matrix is strictly positive definite for Inverse Multiquadrics, Gaussians, and is conditionally positive definite for Multiquadrics under the condition $M' \geq 1$. Hence, for ease of

computing the weighted coefficients, we take $M' = 0$ for Inverse Multiquadrics, Gaussians, and $M' = 1$ for Multiquadrics, in which case, the solvability of Eqs. (13)-(14) is guaranteed beyond all doubt. For Inverse Multiquadrics and Gaussians, the approximate solution can be expressed by $u(\mathbf{x}, t) \cong \sum_{k=0}^M \lambda_k \varphi_k(\mathbf{x})$. According to Eqs. (11)-(12), we easily know that the DQ formulations for fractional directional derivatives are as follows

$$\mathcal{D}_\theta^\alpha \varphi_k(\mathbf{x}_i) = \sum_{j=0}^M \omega_{ij}^{(\alpha)} \varphi_k(\mathbf{x}_j), \quad i, k = 0, 1, \dots, M,$$

obtained by directly replacing $\phi_k(\mathbf{x})$ by $\varphi_k(\mathbf{x})$ in Eqs. (11), which further lead to the below solvable matrix-vector system:

$$\begin{pmatrix} \varphi_0(\mathbf{x}_0) & \varphi_0(\mathbf{x}_1) & \cdots & \varphi_0(\mathbf{x}_M) \\ \varphi_1(\mathbf{x}_0) & \varphi_1(\mathbf{x}_1) & \cdots & \varphi_1(\mathbf{x}_M) \\ \vdots & \vdots & \ddots & \vdots \\ \varphi_M(\mathbf{x}_0) & \varphi_M(\mathbf{x}_1) & \cdots & \varphi_M(\mathbf{x}_M) \end{pmatrix} \begin{pmatrix} \omega_{i0}^{(\alpha)} \\ \omega_{i1}^{(\alpha)} \\ \vdots \\ \omega_{iM}^{(\alpha)} \end{pmatrix} = \begin{pmatrix} \mathcal{D}_\theta^\alpha \varphi_0(\mathbf{x}_i) \\ \mathcal{D}_\theta^\alpha \varphi_1(\mathbf{x}_i) \\ \vdots \\ \mathcal{D}_\theta^\alpha \varphi_M(\mathbf{x}_i) \end{pmatrix}, \quad (15)$$

with $i = 0, 1, \dots, M$ and the coefficient matrix being fully positive definite. As for Multiquadrics, the polynomial term is required to be kept so as to remedy the well-posedness of the algebraic problem. Remembering that $M' = 1$, there hold $u(\mathbf{x}, t) \cong \sum_{k=0}^M \lambda_k \varphi_k(\mathbf{x}) + \lambda_{M+1}$ and the orthogonality condition $\sum_{k=1}^M \lambda_k = 0$. Integrate these two equations into a unified formula to get

$$u(\mathbf{x}, t) \cong \sum_{k=1}^M \lambda_k [\varphi_k(\mathbf{x}) - \varphi_0(\mathbf{x})] + \lambda_{M+1}.$$

According to Eqs. (11)-(12), one then has

$$\mathcal{D}_\theta^\alpha [\varphi_k(\mathbf{x}_i) - \varphi_0(\mathbf{x}_i)] = \sum_{j=0}^M \omega_{ij}^{(\alpha)} [\varphi_k(\mathbf{x}_j) - \varphi_0(\mathbf{x}_j)], \quad i = 0, 1, \dots, M, \quad (16)$$

for $k = 1, 2, \dots, M$, while for $k = 0$, it suffices to show

$$\sum_{j=0}^M \omega_{ij}^{(\alpha)} = 0, \quad (17)$$

owing to $\mathcal{D}_\theta^\alpha C = 0$, with C being a constant. Rearranging Eqs. (16)-(17) in matrix-vector forms, a series of linear system of equations are finally obtained:

$$\mathbf{A} \boldsymbol{\omega}_i^{(\alpha)} = \mathbf{D}_\theta^\alpha \boldsymbol{\varphi}(\mathbf{x}_i) - \mathbf{D}_\theta^\alpha \varphi_0(\mathbf{x}_i), \quad i = 0, 1, \dots, M, \quad (18)$$

where

$$\mathbf{A} = \begin{pmatrix} 1 & 1 & \cdots & 1 \\ \varphi_1(\mathbf{x}_0) - \varphi_0(\mathbf{x}_0) & \varphi_1(\mathbf{x}_1) - \varphi_0(\mathbf{x}_1) & \cdots & \varphi_1(\mathbf{x}_M) - \varphi_0(\mathbf{x}_M) \\ \vdots & \vdots & \ddots & \vdots \\ \varphi_M(\mathbf{x}_0) - \varphi_0(\mathbf{x}_0) & \varphi_M(\mathbf{x}_1) - \varphi_0(\mathbf{x}_1) & \cdots & \varphi_M(\mathbf{x}_M) - \varphi_0(\mathbf{x}_M) \end{pmatrix},$$

$$\boldsymbol{\omega}_i^{(\alpha)} = \begin{pmatrix} \omega_{i0}^{(\alpha)} \\ \omega_{i1}^{(\alpha)} \\ \vdots \\ \omega_{iM}^{(\alpha)} \end{pmatrix}, \quad \mathbf{D}_\theta^\alpha \boldsymbol{\varphi}(\mathbf{x}_i) = \begin{pmatrix} \mathcal{D}_\theta^\alpha \varphi_0(\mathbf{x}_i) \\ \mathcal{D}_\theta^\alpha \varphi_1(\mathbf{x}_i) \\ \vdots \\ \mathcal{D}_\theta^\alpha \varphi_M(\mathbf{x}_i) \end{pmatrix}, \quad \mathbf{D}_\theta^\alpha \boldsymbol{\varphi}_0(\mathbf{x}_i) = \begin{pmatrix} \mathcal{D}_\theta^\alpha \varphi_0(\mathbf{x}_i) \\ \mathcal{D}_\theta^\alpha \varphi_0(\mathbf{x}_i) \\ \vdots \\ \mathcal{D}_\theta^\alpha \varphi_0(\mathbf{x}_i) \end{pmatrix}.$$

The unknown $\boldsymbol{\omega}_i^{(\alpha)}$, $i = 0, 1, \dots, M$, are the weighted vectors what we seek for. However, here arises another question of how to compute each component of the right-hand vectors $\mathbf{D}_\theta^\alpha \boldsymbol{\varphi}(\mathbf{x}_i)$, $\mathbf{D}_\theta^\alpha \boldsymbol{\varphi}_0(\mathbf{x}_i)$, which are the keys to formulating Eqs. (15), (18). Generally, the explicit expressions for the fractional derivatives of a function can be derived but limited to a very small part of functions, that is to say, in most cases, the explicit expressions are not available, hence the explicit expressions should not be anticipated here, neither are the general numerical quadrature rules since the weakly singular integral structure in fractional derivatives. In the sequel, we approximate the fractional directional derivatives $\mathbf{D}_\theta^\alpha \boldsymbol{\varphi}(\mathbf{x}_i)$, $\mathbf{D}_\theta^\alpha \boldsymbol{\varphi}_0(\mathbf{x}_i)$ by using Gauss-Jacobi quadrature rules in a similar way as it is done for the fractional directional integration after making a suitable integral transformation [31]. At first, consider the components of $\mathbf{D}_\theta^\alpha \boldsymbol{\varphi}(\mathbf{x}_i)$ with $\varphi_k(\mathbf{x}_i)$, $k = 0, 1, \dots, M$, being the Inverse Multiquadrics. In view of the definition of integer-order directional derivative, one has

$$\mathcal{D}_\theta^2 \varphi_k(\mathbf{x}) = \cos^2 \theta \frac{\partial^2 \varphi(x, y)}{\partial x^2} + \sin^2 \theta \frac{\partial^2 \varphi(x, y)}{\partial y^2} + 2 \sin \theta \cos \theta \frac{\partial^2 \varphi(x, y)}{\partial x \partial y},$$

with $0 \leq \theta < 2\pi$, $k = 0, 1, \dots, M$, which results in

$$\begin{aligned} \mathcal{D}_\theta^2 \varphi_k(\mathbf{x}) &= \frac{3 \cos^2 \theta (x - x_k)^2 + 3 \sin^2 \theta (y - y_k)^2 + 6 \sin \theta \cos \theta (x - x_k)(y - y_k)}{((x - x_k)^2 + (y - y_k)^2 + \epsilon^2)^{5/2}} \\ &\quad - \frac{1}{((x - x_k)^2 + (y - y_k)^2 + \epsilon^2)^{3/2}}. \end{aligned} \quad (19)$$

On the other hand, by the identity (4), there exists

$$\mathcal{D}_\theta^\alpha \varphi_k(\mathbf{x}) = \frac{1}{\Gamma(2 - \alpha)} \int_0^{z(x, y, \theta)} \omega^{1-\alpha} \mathcal{D}_\theta^2 \varphi(x - \omega \cos \theta, y - \omega \sin \theta) d\omega, \quad (20)$$

with $0 \leq \theta < 2\pi$ and $k = 0, 1, \dots, M$. Doing the integral transformation $\omega = x - 0.5z(x, y, \theta)(1 + \varsigma)$ in Eq. (20), it is not difficulty to check

$$\mathcal{D}_\theta^\alpha \varphi_k(\mathbf{x}) = \frac{1}{\Gamma(2 - \alpha)} \left(\frac{z(x, y, \theta)}{2} \right)^{2-\alpha} \int_{-1}^1 (1 + \varsigma)^{1-\alpha} \chi(x, y, \theta, \varsigma) d\varsigma, \quad (21)$$

where

$$\chi(x, y, \theta, \varsigma) = \mathcal{D}_\theta^2 \varphi \left(x - \cos \theta \frac{z(x, y, \theta)(1 + \varsigma)}{2}, y - \sin \theta \frac{z(x, y, \theta)(1 + \varsigma)}{2} \right),$$

which turns out to be a special form of integration as

$$\int_{-1}^1 (1-\xi)^\lambda (1+\xi)^\mu f(\xi) d\xi, \quad \lambda, \mu > -1,$$

with $\lambda = 0$ and $\mu = 1 - \alpha$, therefore the values of $\mathcal{D}_\theta^\alpha \varphi_k(\mathbf{x}_i)$, $i, k = 0, 1, \dots, M$, can be approximated by Gauss-Jacobi quadrature rules. Let $\{c_s\}_{s=1}^Q, \{w_s\}_{s=1}^Q$ be the quadrature points and weights. Then, from Eq. (19), it follows that

$$\mathcal{D}_\theta^\alpha \varphi_k(\mathbf{x}_i) \cong \frac{1}{\Gamma(2-\alpha)} \left(\frac{z(x, y, \theta)}{2} \right)^{2-\alpha} \sum_{s=1}^Q w_s \eta(x_i, y_i, c_s), \quad (22)$$

where

$$\eta(x_i, y_i, c_s) = \frac{3 \cos^2 \theta r_x^2 + 3 \sin^2 \theta r_y^2 + 6 \sin \theta \cos \theta r_x r_y}{(r_x^2 + r_y^2 + \epsilon^2)^{5/2}} - \frac{1}{(r_x^2 + r_y^2 + \epsilon^2)^{3/2}},$$

with the following quantities

$$\begin{aligned} r_x &= x_i - \cos \theta \frac{z(x, y, \theta)(1 + c_s)}{2} - x_k, \\ r_y &= y_i - \sin \theta \frac{z(x, y, \theta)(1 + c_s)}{2} - y_k. \end{aligned}$$

In particular, when $\theta = 0, \pi$, Eq. (4) yields the ones in x -axis. Doing the integral transformations $\omega = x - 0.5\Gamma_1(x, y)(1 + \varsigma)$ and $\omega = x + 0.5\Gamma_2(x, y)(1 + \varsigma)$ in Eqs. (5)-(6), respectively, $\mathcal{D}_0^\alpha \varphi_k(\mathbf{x})$, $\mathcal{D}_\pi^\alpha \varphi_k(\mathbf{x})$ simply become

$$\begin{aligned} \mathcal{D}_0^\alpha \varphi_k(\mathbf{x}) &= \frac{1}{\Gamma(2-\alpha)} \left(\frac{x-a}{2} \right)^{2-\alpha} \int_{-1}^1 (1+\varsigma)^{1-\alpha} \varphi_k^{(2)} \left(x - \frac{(x-a)(1+\varsigma)}{2}, y \right) d\varsigma, \\ \mathcal{D}_\pi^\alpha \varphi_k(\mathbf{x}) &= \frac{1}{\Gamma(2-\alpha)} \left(\frac{b-x}{2} \right)^{2-\alpha} \int_{-1}^1 (1+\varsigma)^{1-\alpha} \varphi_k^{(2)} \left(x + \frac{(b-x)(1+\varsigma)}{2}, y \right) d\varsigma, \end{aligned}$$

with $a = \Gamma_1(x, y)$ and $b = \Gamma_2(x, y)$. Then, the computational formulas for $\mathcal{D}_0^\alpha \varphi_k(\mathbf{x}_i)$, $\mathcal{D}_\pi^\alpha \varphi_k(\mathbf{x}_i)$, $i, k = 1, 2, \dots, M$, are obtained as below

$$\mathcal{D}_0^\alpha \varphi_k(\mathbf{x}_i) \cong \frac{1}{\Gamma(2-\alpha)} \left(\frac{x_i - a}{2} \right)^{2-\alpha} \sum_{s=1}^Q w_s \eta_0 \left(x_i - \frac{(x_i - a)(1 + c_s)}{2}, y_i \right), \quad (23)$$

$$\mathcal{D}_\pi^\alpha \varphi_k(\mathbf{x}_i) \cong \frac{1}{\Gamma(2-\alpha)} \left(\frac{b - x_i}{2} \right)^{2-\alpha} \sum_{s=1}^Q w_s \eta_0 \left(x_i + \frac{(b - x_i)(1 + c_s)}{2}, y_i \right), \quad (24)$$

where

$$\eta_0(x, y, c_s) = \frac{3(x - x_k)^2}{((x - x_k)^2 + (y - y_k)^2 + \epsilon^2)^{5/2}} - \frac{1}{((x - x_k)^2 + (y - y_k)^2 + \epsilon^2)^{3/2}}.$$

As for Gaussians and Multiquadrics, along the same line, we can derive a unified computational formula similar to (22) for $\mathcal{D}_\theta^\alpha \varphi_k(\mathbf{x}_i)$, but with

$$\eta(x_i, y_i, c_s) = 2\epsilon^2 e^{-\epsilon^2 r_x^2 - \epsilon^2 r_y^2} (2 \cos^2 \theta r_x^2 + 2 \sin^2 \theta r_y^2 + 4 \sin \theta \cos \theta r_x r_y - 1),$$

for Gaussians and

$$\eta(x_i, y_i, c_s) = \frac{1}{(r_x^2 + r_y^2 + \epsilon^2)^{1/2}} - \frac{\cos^2 \theta r_x^2 + \sin^2 \theta r_y^2 + 2 \sin \theta \cos \theta r_x r_y}{(r_x^2 + r_y^2 + \epsilon^2)^{3/2}}$$

for Multiquadrics. Here, r_x, r_y are the quantities defined as before. In particular, if θ is taken to be $0, \pi$, doing the same manner as before, two formulas for the fractional derivatives in x -axis as (23)-(24) are obtained, but with

$$\eta_0(x, y, c_s) = 2\epsilon^2 e^{-\epsilon^2 (x-x_k)^2 - \epsilon^2 (y-y_k)^2} (2(x-x_k)^2 - 1),$$

$$\eta_0(x, y, c_s) = \frac{1}{((x-x_k)^2 + (y-y_k)^2 + \epsilon^2)^{1/2}} - \frac{(x-x_k)^2}{((x-x_k)^2 + (y-y_k)^2 + \epsilon^2)^{3/2}},$$

for these two kinds of RBFs, respectively. Once getting $\mathbf{D}_\theta^\alpha \varphi(\mathbf{x}_i)$, $\mathbf{D}_\theta^\alpha \varphi_0(\mathbf{x}_i)$, $i = 0, 1, \dots, M$, the weighted vectors $\omega_i^{(\alpha)}$ are determined by solving Eqs. (15), (18) for each nodal point \mathbf{x}_i and the fractional directional derivatives are then eliminated from a fractional PDE by using Eqs. (11) as replacements, thus we can obtain the approximate solutions by solving ODEs instead.

4 Time-stepping DQ methods and implemental processes

In this section, we propose time-stepping DQ methods to approximate the solutions of Eqs. (7)-(9) and show the implemental procedures. Define a lattice on $[0, T]$ with equally spaced points $t_n = n\tau$, $\tau = T/N$, $N \in \mathbb{Z}^+$, and denote by $\omega_{ij}^{(\alpha)}$, $i, j = 0, 1, \dots, M$, the weighted coefficients of $\mathcal{D}_\theta^{\alpha_i} u(\mathbf{x})$. On inserting the weighted sums (11) into Eq. (7), we have the first-order ODEs:

$$\frac{\partial u(\mathbf{x}_i, t)}{\partial t} - \sum_{l=1}^L \kappa_l(\mathbf{x}_i) \sum_{j=0}^M a_{ij}^{(\alpha_l)} u(\mathbf{x}_j, t) = f(\mathbf{x}_i, t), \quad i = 0, 1, \dots, M.$$

Discretizing the ODEs by the Crank-Nicolson scheme reaches to

$$u(\mathbf{x}_i, t_n) - \frac{\tau}{2} \sum_{l=1}^L \kappa_l(\mathbf{x}_i) \sum_{j=0}^M a_{ij}^{(\alpha_l)} u(\mathbf{x}_j, t_n) = u(\mathbf{x}_i, t_{n-1})$$

$$+ \frac{\tau}{2} \sum_{l=1}^L \kappa_l(\mathbf{x}_i) \sum_{j=0}^M a_{ij}^{(\alpha_l)} u(\mathbf{x}_j, t_{n-1}) + \tau f\left(\mathbf{x}_i, t_n - \frac{\tau}{2}\right), \quad (25)$$

associated with the boundary constraints

$$u(\mathbf{x}_i, t) = g(\mathbf{x}_i, t_n), \quad \text{for all } \mathbf{x}_i \in \partial\Omega, \quad (26)$$

where $i = 0, 1, \dots, M$. The initial state are directly got from Eq. (8). In order to avoid wordy expressions below, we adopt $t_{n-1/2} = t_n - \frac{\tau}{2}$, $\kappa_i = \kappa(\mathbf{x}_i, t_n)$, $u_i^n = u(\mathbf{x}_i, t_n)$, $g_i^n = g(\mathbf{x}_i, t_n)$, and $f_i^{n-1/2} = f(\mathbf{x}_i, t_{n-1/2})$. Rewriting Eqs. (25)-(26) in matrix-vector form, we finally obtain the fully discrete scheme

$$\left(\mathbf{I} - \frac{\tau}{2} \sum_{l=1}^L \kappa_l \mathbf{W}_l\right) \mathbf{U}^n = \left(\mathbf{I} + \frac{\tau}{2} \sum_{l=1}^L \kappa_l \mathbf{W}_l\right) \mathbf{U}^{n-1} + \tau \mathbf{F}^{n-1/2}, \quad (27)$$

associated with the boundary constraints

$$u(\mathbf{x}_i, t) = g(\mathbf{x}_i, t_n), \quad \text{for all } \mathbf{x}_i \in \partial\Omega, \quad (28)$$

where \mathbf{I} is the $(M+1) \times (M+1)$ identity matrix, $\mathbf{U}^n = [u_0^n, u_1^n, \dots, u_M^n]^T$, $\kappa_l = \text{diag}(\kappa_0^l, \kappa_1^l, \dots, \kappa_M^l)$, and $\mathbf{W}_l, \mathbf{H}^{n-1/2}$ are given by

$$\mathbf{W}_l = \begin{pmatrix} \omega_{00}^{(\alpha_l)} & \omega_{01}^{(\alpha_l)} & \cdots & \omega_{0M}^{(\alpha_l)} \\ \omega_{10}^{(\alpha_l)} & \omega_{11}^{(\alpha_l)} & \cdots & \omega_{1M}^{(\alpha_l)} \\ \vdots & \vdots & \ddots & \vdots \\ \omega_{M0}^{(\alpha_l)} & \omega_{M1}^{(\alpha_l)} & \cdots & \omega_{MM}^{(\alpha_l)} \end{pmatrix}, \quad \mathbf{F}^{n-1/2} = \begin{pmatrix} f_0^{n-1/2} \\ f_1^{n-1/2} \\ \vdots \\ f_M^{n-1/2} \end{pmatrix}.$$

In what follows, we show a detailed algorithm on how to implement Eqs. (27)-(28). Our codes are written in Matlab 2012a and for the ease of exposition, some commands will be acquiescently used as notations if no ambiguity is possible, for instance, $\mathbf{A}(k, l)$ means extracting the element from the matrix \mathbf{A} , which locates at Rank k and Column l , if the corresponding element exists. Let $nonb$, $boup$ be the index of the internal and boundary nodal points on Ω , respectively. Also, let $\tilde{\mathbf{U}}^n$ be the unknowns related to the internal nodal points, i.e., $\mathbf{U}^n(nonb)$. Then Eqs. (27)-(28) can be integrated into a unified form

$$\left(\tilde{\mathbf{I}} - \frac{\tau}{2} \sum_{l=1}^L \tilde{\kappa}_l \mathbf{K}_l\right) \tilde{\mathbf{U}}^n = \left(\tilde{\mathbf{I}} + \frac{\tau}{2} \sum_{l=1}^L \tilde{\kappa}_l \mathbf{K}_l\right) \tilde{\mathbf{U}}^{n-1} + \tau \mathbf{H}^{n-1/2}, \quad (29)$$

where $\tilde{\mathbf{I}}$ is the identity matrix of rank $length(nonb)$, $\tilde{\kappa}_l = \kappa_l(nonb)$, $\mathbf{K}_l = \mathbf{W}_l(nonb, nonb)$, and the right-hand vector

$$\mathbf{H}^{n-1/2} = \tilde{\mathbf{F}}^{n-1/2} + \frac{1}{2} \sum_{p=1}^P \sum_{l=1}^L (\tilde{\mathbf{g}}^n + \tilde{\mathbf{g}}^{n-1}) \mathbf{G}(:, p), \quad (30)$$

with $P = length(boup)$, $\tilde{\mathbf{g}}^n = \mathbf{g}^n(nonb)$, $\tilde{\mathbf{F}}^{n-1/2} = \mathbf{F}^{n-1/2}(nonb)$, $\mathbf{G}_l = \mathbf{W}_l(nonb, boup)$, and $\mathbf{g}^n = [g_0^n, g_1^n, \dots, g_M^n]^T$. An detailed implementation of the algorithm for Eqs. (29)-(30) is summarized in the following flowchart

1. Input $\alpha_l, \theta_l, \epsilon, M, N$, and allocate $\{t_n\}_{n=0}^N, \{\mathbf{x}_i\}_{i=0}^M$
2. Define two zero matrices \mathbf{U}, \mathbf{W}_l and form \mathbf{A}, κ_l
3. while $i \leq M$ do
4. identify the distance $z(x_i, y_i, \theta)$ for each \mathbf{x}_i

5. compute $\mathbf{D}_{\theta_l}^{\alpha_l} \varphi(\mathbf{x}_i)$, $\mathbf{D}_{\theta_l}^{\alpha_l} \varphi_0(\mathbf{x}_i)$ by the formulas (22)-(24) for each \mathbf{x}_i
6. solve Eqs. (15), (18) to obtain $\omega_i^{(\alpha_l)}$ and set $\mathbf{W}_l(i+1, :) = \omega_i^{(\alpha_l)}$
7. end while
8. Let $\tilde{\mathbf{K}}_l = \mathbf{K}_l(\text{nonb})$, $\mathbf{K}_l = \mathbf{W}_l(\text{nonb}, \text{nonb})$, and $\mathbf{G}_l = \mathbf{W}_l(\text{nonb}, \text{boup})$
9. while $n \leq N$ do
10. compute $\tilde{\mathbf{F}}^{n-1/2}$ and set $\tilde{\mathbf{H}}^{n-1/2} = \tilde{\mathbf{F}}^{n-1/2}$
11. compute \mathbf{g}^n , \mathbf{g}^{n-1} and set $\tilde{\mathbf{g}}^n = \mathbf{g}^n(\text{nonb})$, $\tilde{\mathbf{g}}^{n-1} = \mathbf{g}^{n-1}(\text{nonb})$
12. while $p \leq \text{length}(\text{boup})$ do
13. $\tilde{\mathbf{H}}^{n-1/2} = \tilde{\mathbf{H}}^{n-1/2} + \frac{1}{2} \sum_{l=1}^L (\tilde{\mathbf{g}}^n + \tilde{\mathbf{g}}^{n-1}) * \mathbf{G}_l(:, p)$
14. end while
15. $\tilde{\mathbf{U}}^n = \left(\left(\tilde{\mathbf{I}} + \frac{\tau}{2} \sum_{l=1}^L \tilde{\mathbf{K}}_l \mathbf{K}_l \right) \tilde{\mathbf{U}}^{n-1} + \tau \mathbf{H}^{n-1/2} \right) \setminus \left(\tilde{\mathbf{I}} - \frac{\tau}{2} \sum_{l=1}^L \tilde{\mathbf{K}}_l \mathbf{K}_l \right)$
16. $\mathbf{U}(\text{nonb}, n) = \tilde{\mathbf{U}}^n$, $\mathbf{U}(\text{boup}, n) = \mathbf{g}^n$
17. end while
18. Output \mathbf{U} and terminate program

It is visible that our algorithm is truly free of troublesome mesh generation, so are the background cells in meshless Galerkin methods; all the informations need about the scatter points are their co-ordinates, which may make sense to treat the fractional equations as the models we consider here, especially for high-dimensional problems. Moreover, all involved RBFs are $C^\infty(\mathbb{R}^2)$ and this is a sufficient condition that ensures the existence of $D_\theta^\alpha \varphi_k(\mathbf{x}_i)$, $i = 0, 1, \dots, M$.

5 Illustrated examples

In this part, a couple of illustrated examples are carried out to gauge the practical performance of our algorithm, including two 1D problems and the 2D problems on the square, trapezoidal, and circular domains. For simplicity, we abbreviate our methods to MQ-DQ, IM-DQ, and GA-DQ methods in the order of first appearance of the RBFs we use. In the computation, the algorithm in [15] is applied to generate the Gauss-Jacobi quadrature points and weights and 50 quadrature points and weights are preferred in calculating the weighted coefficients. As to the shape parameter, how to choose it is still be open, although continued efforts have been devoted to theoretically or numerically seek its optimal value for interpolation [7, 10, 17, 24, 38, 41], at which, the errors are minimum. One thing we have to bear in mind is that its value would markedly affect the accuracy of RBFs-based methods, which is a principle also working for the DQ methods. Since the shape parameter should be adjusted with the nodal number M , we artificially determine ϵ and also use $\epsilon = c^*/(M+1)^{0.25}$ in 2D cases as some works did with $c^* \geq 0$. During the entire computational processes, the numerical errors are measured by

$$e_2(t, M) = \sqrt{\frac{1}{M+1} \sum_{j=0}^M |u_j^n - U_j^n|^2}, \quad e_\infty(t, M) = \max_{0 \leq j \leq M} |u_j^n - U_j^n|,$$

Table 1 The numerical results with $\alpha = 1.2$ and $\beta = 3$ for Example 5.1

M	MQ-DQ method		IM-DQ method		GA-DQ method	
	$e_2(t, M)$	$e_\infty(t, M)$	$e_2(t, M)$	$e_\infty(t, M)$	$e_2(t, M)$	$e_\infty(t, M)$
10	2.5459e-02	4.7254e-02	3.8207e-02	6.2084e-02	9.3444e-02	1.5869e-01
15	9.8161e-03	2.0683e-02	1.1916e-02	2.5528e-02	3.2316e-02	7.0755e-02
20	4.8985e-03	1.1519e-02	6.1154e-03	1.3830e-02	1.6083e-02	3.8576e-02
25	2.8489e-03	7.1813e-03	3.5079e-03	8.5431e-03	9.5893e-03	2.4149e-02

and the corresponding convergent rates are computed by

$$\text{Cov. rate} = \frac{\log_2(e_\nu(t, M_1)/e_\nu(t, M_2))}{\log_2(M_2/M_1)}, \quad \nu = 2, \infty,$$

where u_j^n, U_j^n denote the exact and numerical solutions on the nodal point \mathbf{x}_j at the time level n , respectively. For 1D problems, we perform the algorithm on the nodal distribution $x_j = 0.5(1 - \cos \frac{j\pi}{M})\ell + a$, $\ell = b - a$, $j = 0, 1, \dots, M$, on the computational interval $[a, b]$, while for 2D problems, both regularly and irregularly nodal distributions would be used for tests.

Example 5.1. Approximate the fractional derivative $D_\pi^\alpha(1 - x)^\beta$ on the interval $[0, 1]$. From the basic property of fractional derivative, we have

$$D_\pi^\alpha(1 - x)^\beta = \frac{\Gamma(\beta + 1)}{\Gamma(\beta + 1 - \alpha)}(1 - x)^{\beta - \alpha}.$$

In order to show the effectiveness of the DQ formulations, we place 11, 16, 21, and 26 nodal points on the computational interval, respectively, and select their corresponding ϵ for Multiquadrics by 0.3112, 0.2150, 0.1678, 0.1374, and for Inverse Multiquadrics by 0.4327, 0.3328, 0.2694, and 0.2255. As for Gaussians, we employ the data sets consisting of 4.0381, 5.3768, 6.6514, and 7.8994. The computing errors for $\alpha = 1.2$ and $\beta = 3$ are tabulated in Table 1. Here, the approximations improve as M increases, which implies that the new DQ formulations are valid. Besides, under these ϵ 's, MQ-DQ formulation is more efficient than IM-DQ and GA-DQ formulations in term of accuracy.

Example 5.2. Letting $\theta = 0$, consider the fractional diffusion equation

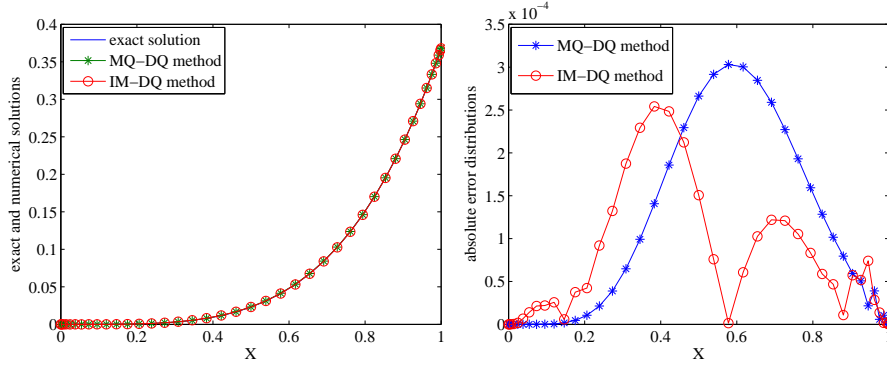
$$\frac{\partial u(x, t)}{\partial t} - \frac{x^\alpha \Gamma(5 - \alpha)}{24} D_\theta^\alpha u(x, t) = -2e^{-t}x^4,$$

on the interval $[0, 1]$, subjected to the initial and boundary conditions $u(x, 0) = x^4$, $u(0, t) = 0$, and $u(1, t) = e^{-t}$. It is verified that the exact solution is $u(x, t) = e^{-t}x^4$. As the first example, we place 16, 21, 26, and 31 nodal points on the interval, respectively, and artificially select ϵ by 0.1875, 0.1128, 0.0712, 0.0613 for Multiquadrics and by 0.3098, 0.2135, 0.1567, and 0.1149 for Inverse Multiquadrics. Taking $N = M$, the numerical results of MQ-DQ and IM-DQ methods at $t = 1$ for $\alpha = 1.5$ are compared with those obtained by SAM [43],

Table 2 A comparison of SAM and our DQ methods at $t = 1$ for $N = M$ and $\alpha = 1.5$.

M	SAM [43]		MQ-DQ method		IM-DQ method	
	$e_\infty(t, M)$	Cov. rate	$e_\infty(t, M)$	Cov. rate	$e_\infty(t, M)$	Cov. rate
15	7.660e-04	-	2.5379e-04	-	2.9346e-04	-
20	4.493e-04	1.9	1.3366e-04	2.2288	1.5818e-04	2.1483
25	2.929e-04	1.9	8.2231e-05	2.1770	9.8308e-05	2.1315
30	2.067e-04	1.9	5.5969e-05	2.1102	6.6635e-05	2.1329

all of which are presented side by side in Table 2. Resetting $\epsilon = 0.0312$ for Multiquadrics and $\epsilon = 0.0511$ for Inverse Multiquadrics, we display the exact and numerical solutions at $t = 1$ with $M = 40$ in Fig. 2 (left) and the absolute error distributions in Fig. 2 (right). As seen from these table and graphs, our methods yield the approximations well agreeing with the exact solution and produce less errors than SAM; furthermore, the computational accuracy not only relies on the nodal number M but also the shape parameter ϵ .

**Fig. 2** The exact and numerical solutions (left) and absolute error distributions (right) at $t = 1$ by using $M = 40$ and $\epsilon = 0.0312, 0.0511$ for MQ-DQ and IM-DQ methods, respectively.

Example 5.3. Consider the 2D fractional diffusion equation

$$\frac{\partial u(x, y, t)}{\partial t} - \kappa_1(x, y) D_{\theta_1}^{\alpha_1} u(x, y, t) - \kappa_2(x, y) D_{\theta_2}^{\alpha_2} u(x, y, t) = f(x, y, t),$$

on the square domain $[0, 1] \times [0, 1]$ in two separate cases. The former uses the regularly distributed nodal points while the latter chooses the irregularly distributed nodal points. To compare with the FDM proposed in [26], we arrange the computational parameters in the following two cases:

- (i) Letting $\alpha_1 = 1.8$, $\alpha_2 = 1.6$, $\theta_1 = 0$, $\theta_2 = \pi/2$, $\kappa_1(x, y) = \frac{\Gamma(2.2)x^{2.8}y}{6}$, $\kappa_2(x, y) = \frac{2xy^{2.6}}{\Gamma(4.6)}$, and the source function $f(x, y, t) = -(1 + 2xy)e^{-t}x^3y^{3.6}$, solve the above equation with the initial and boundary conditions $\varphi(x, y) =$

Table 3 A comparison of FDM and our DQ methods at $t = 1$ when $N = \sqrt{M+1} - 1$.

M	FDM [26]		M	MQ-DQ method		IM-DQ method	
	$e_\infty(t, M)$	Cov. rate		$e_\infty(t, M)$	Cov. rate	$e_\infty(t, M)$	Cov. rate
120	1.2629e-03	-	99	9.8707e-04	-	2.0189e-03	-
440	6.7325e-04	1.88	195	3.8599e-04	1.3953	9.1539e-04	1.1753
1680	3.4824e-04	1.93	288	2.0239e-04	1.6626	5.3768e-04	1.3703
6560	1.7660e-04	1.97	440	9.4054e-05	1.8133	2.8080e-04	1.5371

$x^3y^{3.6}$, $u(0, y, t) = u(x, 0, t) = 0$, $u(1, y, t) = e^{-t}y^{3.6}$, and $u(x, 1, t) = e^{-t}x^3$.
The exact solution is given by $u(x, y, t) = e^{-t}x^3y^{3.6}$.

- (ii) Letting $\alpha_1 = 1.8$, $\theta_1 = \pi/4$, $\kappa_1(x, y) = x^{\alpha_1}$, $\kappa_2(x, y) = 0$, and the source function $f(x, y, t) = -e^{-t}x^2y^2 - e^{-t}x^{\alpha_1}f^*(x, y, t)$ with

$$f^*(x, y, t) = \begin{cases} \frac{2^{1-\frac{\alpha_1}{2}}y^{2-\alpha_1}\left((\alpha_1-4)(\alpha_1-3)x^2-2(\alpha_1-4)\alpha_1xy+(\alpha_1-1)\alpha_1y^2\right)}{\Gamma(5-\alpha_1)}, & x \geq y, \\ \frac{2^{1-\frac{\alpha_1}{2}}x^{2-\alpha_1}\left((\alpha_1-1)\alpha_1x^2-2(\alpha_1-4)\alpha_1xy+(\alpha_1-4)(\alpha_1-3)y^2\right)}{\Gamma(5-\alpha_1)}, & x < y, \end{cases}$$

solve the above equation with the initial and boundary conditions $\varphi(x, y) = x^2y^2$, $u(0, y, t) = u(x, 0, t) = 0$, $u(1, y, t) = e^{-t}y^2$, and $u(x, 1, t) = e^{-t}x^2$. It can be verified that the exact solution is $u(x, y, t) = e^{-t}x^2y^2$.

In the second case, the source function suffers relatively complex mathematical structure since θ_1 does not along the axis directions. In Table 3, we give a comparison between our methods and FDM in term of maximum errors for the case of (i) with $N = \sqrt{M+1} - 1$, $c^* = 1.17$ for Multiquadrics and $c^* = 1.42$ for Inverse Multiquadrics. The used regular distribution of nodal points as well as its corresponding numerical solution created by MQ-DQ method with $M = 440$ are shown in Fig. 3. For the case of (ii), we list the numerical results of our methods in Table 4 by using the irregular nodal points of total numbers 74, 144, 234, and 424, with $N = 2000$, $c^* = 0.89$ for Multiquadrics and $c^* = 1.25$ for Inverse Multiquadrics. In Fig. 4, we display the used irregular distributions of nodal points, and in Fig. 5, by resetting $M = 518$ and $\epsilon = 8.6924$, we compare the exact and numerical solutions at $t = 1$ created by GA-DQ method. As expected, our methods work well on both regularly and irregularly nodal distributions and yield the approximations that are in good agreement with the exact ones. It is also drawn that our methods achieve the errors in the same scale of magnitude as FDM with less nodal numbers.

Example 5.4. Consider the 2D fractional diffusion equation

$$\frac{\partial u(x, y, t)}{\partial t} - x^{\alpha_1}D_{\theta_1}^{\alpha_1}u(x, y, t) - (1.5 - x - 0.5y)^{\alpha_2-3}D_{\theta_2}^{\alpha_2}u(x, y, t) = f(x, y, t),$$

on the trapezoidal domain as shown in Fig. 6, with $\theta_1 = 0$, $\theta_2 = \pi$, the exact solution $u(x, y, t) = e^{-t}x^3(0.5(3-y)-x)^3$, the source function

$$f(x, y, t) = e^{-t}x^3(x - 0.5(3-y))^3 - e^{-t}(g_1^*(\alpha_1, x, 3-y) + g_2^*(\alpha_2, x, 3-y)),$$

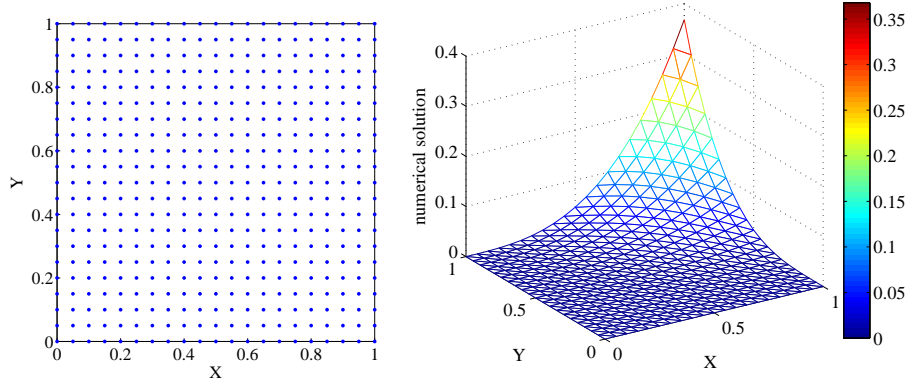


Fig. 3 The nodal distribution with $M = 440$ and numerical solution for MQ-DQ method.

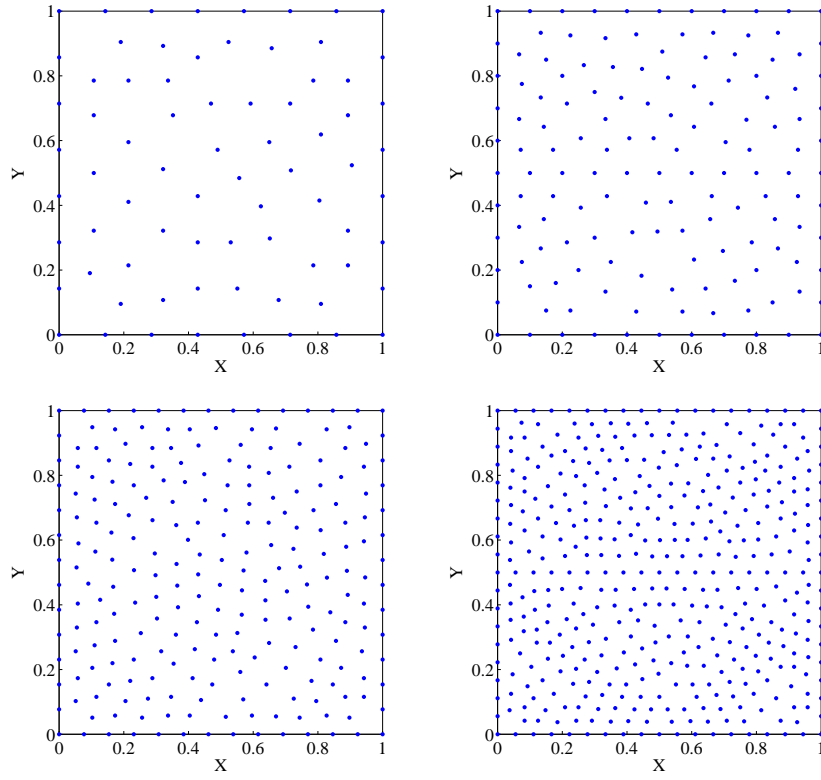


Fig. 4 The nodal distributions with total numbers 74, 144, 234, and 424 for Example 5.3.

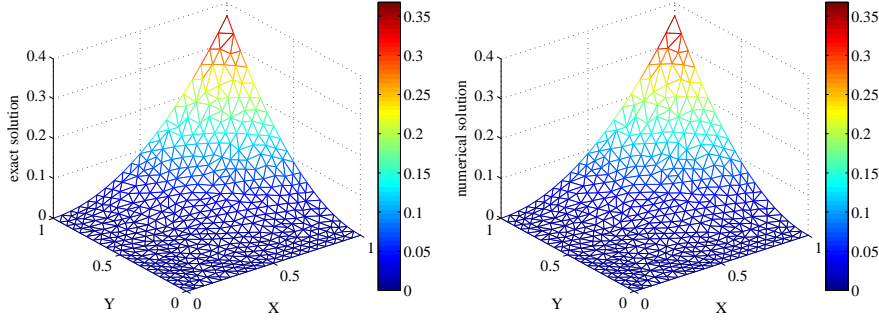
and the initial and boundary conditions taken from $u(x, y, t)$, where

$$g_1^*(\alpha, x, y) = \frac{0.75x^3y^3}{\Gamma(4-\alpha)} - \frac{18x^4y^2}{\Gamma(5-\alpha)} + \frac{180x^5y}{\Gamma(6-\alpha)} - \frac{720x^6}{\Gamma(7-\alpha)},$$

$$g_2^*(\alpha, x, y) = \frac{0.75(\alpha-2)(\alpha-1)\alpha y^3 + 18(\alpha-1)\alpha x y^2 + 180\alpha x^2 y + 720x^3}{\Gamma(7-\alpha)}.$$

Table 4 The numerical results at $t = 1$ with $N = 2000$ and $\alpha = 1.8$ for Example 5.3.

M	MQ-DQ method		IM-DQ method	
	$e_2(t, M)$	Cov. rate	$e_2(t, M)$	Cov. rate
73	4.5310e-04	-	9.5684e-04	-
143	2.6755e-04	0.7913	4.6647e-04	1.0792
233	8.8580e-05	2.2768	1.6103e-04	2.1907
423	2.6730e-05	2.0156	4.7417e-05	2.0568

**Fig. 5** The exact and numerical solutions created by GA-DQ method for Example 5.3.**Table 5** The numerical results at $t = 1$ with $N = 5000$, $\alpha_1 = 1.1$, and $\alpha_2 = 1.3$ for Example 5.4.

M	MQ-DQ method		IM-DQ method	
	$e_\infty(t, M)$	Cov. rate	$e_\infty(t, M)$	Cov. rate
65	1.4714e-03	-	1.3140e-03	-
170	7.8355e-04	0.6619	7.6459e-04	0.5688
286	4.3674e-04	1.1288	4.5347e-04	1.0088
436	2.6449e-04	1.1928	2.7898e-04	1.1554

Let $\alpha_1 = 1.1$, $\alpha_2 = 1.3$, and $N = 5000$. We run the algorithm with $c^* = 1.1$ for Multiquadrics and $c^* = 1.29$ for Inverse Multiquadrics on the irregularly distributed nodal points of total numbers 66, 171, 287, and 437, which are plotted in Fig. 6, respectively. Table 5 reports the errors of the numerical solutions of DQ methods with regard to the exact solution at $t = 1$ at length. It is evident that, under the chosen ϵ 's, the proposed methods are stable and well convergent on this trapezoidal domain. Using the last nodal distribution plotted in Fig. 6 and its corresponding ϵ , a comparison between the exact and numerical solutions at $t = 1$ created by IM-DQ method is presented in Fig. 7, where no obvious difference can be observed from these two graphs.

Example 5.5. In the last test, consider the 2D fractional diffusion equation

$$\frac{\partial u(x, y, t)}{\partial t} - \frac{y^\alpha}{2} D_\theta^\alpha u(x, y, t) = f(x, y, t),$$

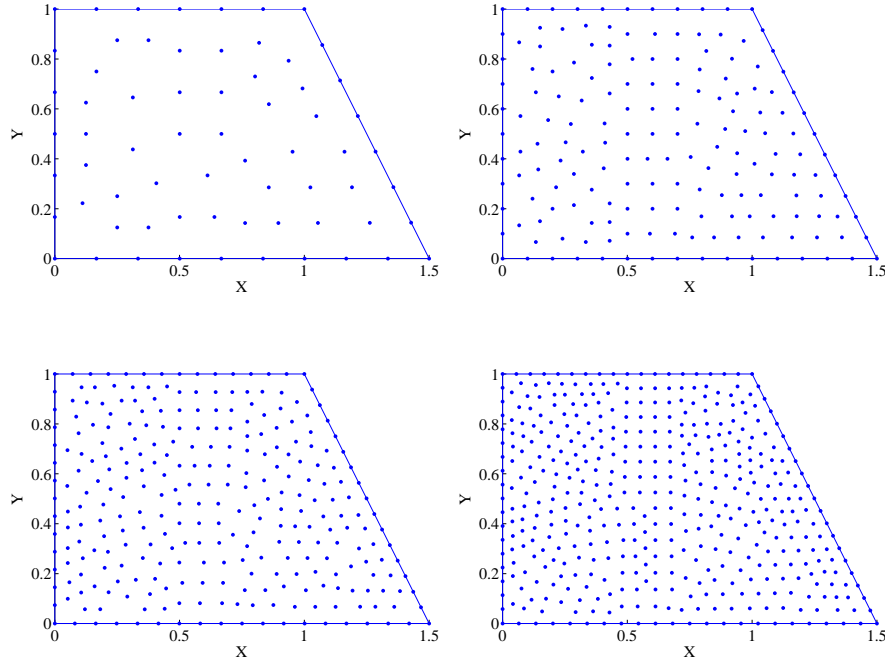


Fig. 6 The nodal distributions with total numbers 66, 171, 287, and 437 for Example 5.4.

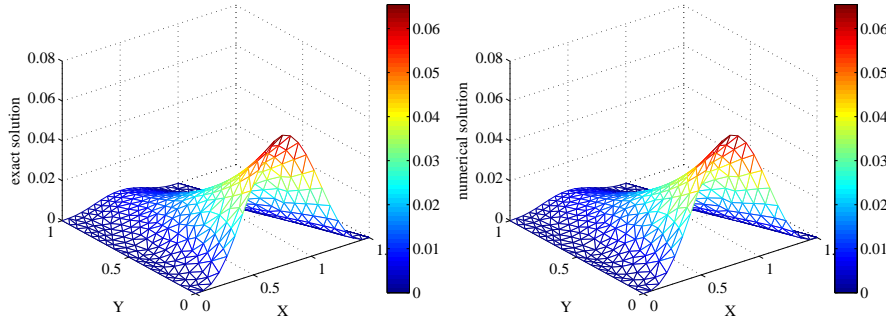


Fig. 7 The exact and numerical solutions created by IM-DQ method for Example 5.4.

on the circular domain $\Omega = \{(x, y) : x^2 + y^2 \leq 1\}$, with $\theta = 0$, the exact solution $u(x, y, t) = t^2(x - (0.5 - \sqrt{0.25 - (y - 0.5)^2})^2 y^2$, the source function

$$f(x, y, t) = 2t(x - (0.5 - \sqrt{0.25 - (y - 0.5)^2})^2 y^2 - \frac{t^2(x - (0.5 - \sqrt{0.25 - (y - 0.5)^2})^2 y^{2+\alpha}}{\Gamma(3 - \alpha)},$$

and the initial and boundary conditions directly taken from the exact solution. The computational domain as well as the involved irregular nodal distributions of total numbers 54, 80, 201, and 402 are displayed in Fig. 8, respectively. To see the actual performance of our methods, we compute the numerical results at $t = 1$ with $N = 5000$ and document them side by side in Table 6 by using $c^* = 1.25$ for Inverse Multiquadrics and the data sets consisting of 4.7716, 5.2643, 6.6278, and 7.8818 for the free parameter contained in Gaussians. It is found that our methods show their capability to deal with the fractional problem on circular domains even if the nodal distributions are irregular. Besides, IM-DQ method outperforms GA-DQ method in term of overall accuracy, of course, this phenomena may appear only under the ϵ 's we select since the shape parameters are important factors that influence their accuracy and convergent rates. Resetting $M = 473$ together with $\epsilon = 8.8553$, we compare the exact and numerical solutions at $t = 1$ created by GA-DQ method in Fig. 9. As observed, the method produce a satisfactory approximation with sufficiently small errors which can not be visually distinguished from the exact one. This further confirms the validity and applicability of our proposed methods.

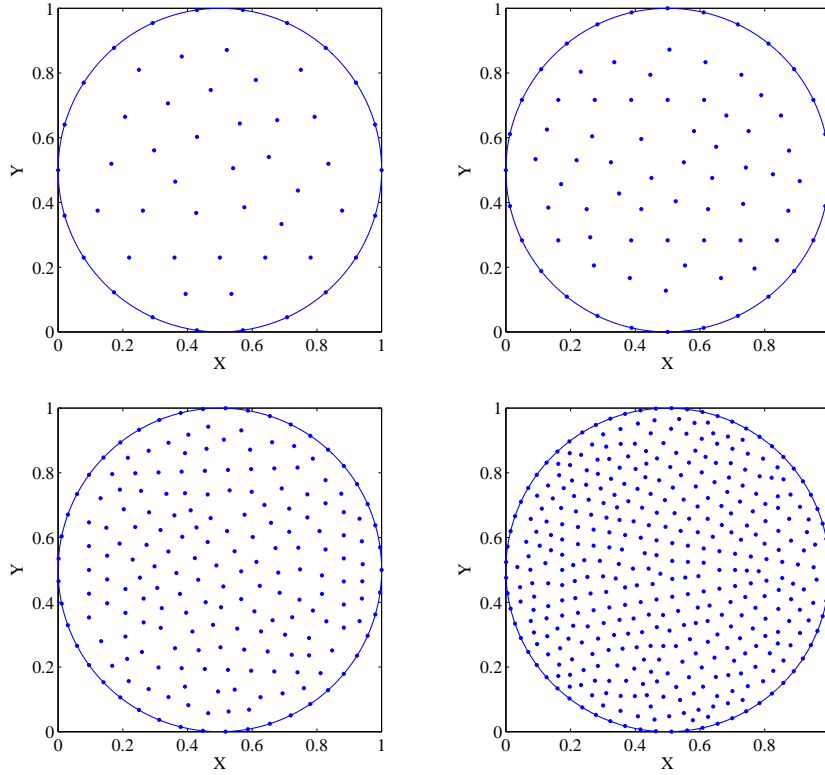
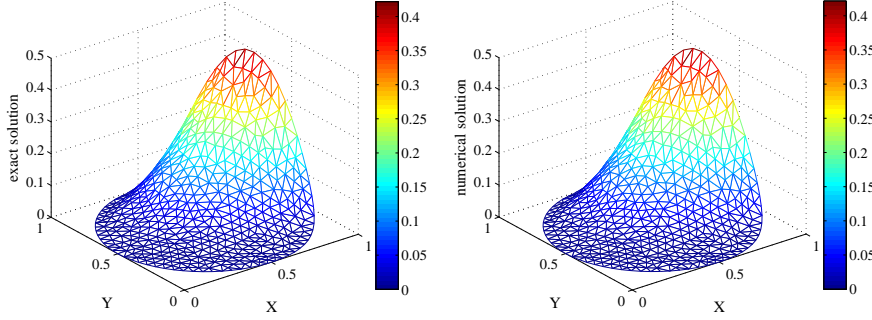


Fig. 8 The nodal distributions with total numbers 54, 80, 201, and 402 for Example 5.5.

Table 6 The numerical results at $t = 1$ with $N = 5000$ and $\alpha = 1.9$ for Example 5.5.

M	IM-DQ method		GA-DQ method	
	$e_2(t, M)$	Cov. rate	$e_2(t, M)$	Cov. rate
53	2.3580e-03	-	9.2964e-03	-
79	1.1662e-03	1.7913	5.9546e-03	1.1334
200	2.8583e-04	1.5263	9.0122e-04	2.0495
401	7.3290e-05	1.9635	3.0539e-04	1.5612

**Fig. 9** The exact and numerical solutions created by GA-DQ method for Example 5.5.

6 Conclusion

The multi-dimensioned space-fractional diffusion equations are known as significant branch of fractional PDEs in mathematical physics, but solving these types of equations appears to be somewhat challenging due to the non-local properties of fractional derivatives, especially on irregular domains. In this research, by using Multiquadric, Inverse Multiquadric and Gaussian RBFs as test functions, the DQ formulations for fractional directional derivatives in Caputo sense are introduced. Then, three effective DQ methods are proposed for the space-fractional diffusion equations on 2D irregular domains via discretizing the resultant ODEs by employing the Crank-Nicolson scheme. The new methods equip with some appealing advantages such as low occupancy cost, truly *mesh-free*, and the ease of programming, which makes they compare favorably to some of the traditional methods as FDM. The computational accuracy relies on the nodal number, shape parameter, the complexity of fractional models, and the other potential factors. The codes are utilized to solve the space-fractional diffusion equations on square, trapezoidal, and circular domains, respectively, and the outcomes have demonstrated that our methods are capable of capturing the exact solutions under the condition that the shape parameters are well prepared. Due to the characteristics of RBFs, these DQ

methods are insensitive to dimensional change, which says that they can be generalized to three-dimensions without a significant increase in computational burden. Such merit obviously provides a possibility for simulating the other complex space-fractional problems on high-dimensional domains with irregular boundaries arising in the areas of anomalous dispersion, fluid dynamics, conservative systems, genetic propagation, and viscoelastic materials.

Acknowledgements This research was supported by National Natural Science Foundations of China (No.11471262 and 11501450).

References

1. Adams, E.E., Gelhar, L.W.: Field study of dispersion in a heterogeneous aquifer: 2. Spatial moments analysis. *Water Res. Research* **28**, 3293–3307 (1992)
2. Alfonso, B.O., David, K., Kevin, B.: Fourier spectral methods for fractional-in-space reaction-diffusion equations. *BIT* **54**(4), 937–954 (2014)
3. Bellman, R., Casti, J.: Differential quadrature and long-term integration. *J. Math. Anal. Appl.* **34**(2), 235–238 (1971)
4. Bellman, R., Kashef, B., Lee, E.S., Vasudevan, R.: Differential quadrature and splines. *Comput. Math. Appl.* **1**(3), 371–376 (1975)
5. Bhrawy, A.H., Baleanu, D.: A spectral Legendre–Gauss–Lobatto collocation method for a space-fractional advection diffusion equations with variable coefficients. *Rep. Math. Phys.* **72**(2), 219–233 (2013)
6. Bonzani, I.: Solution of nonlinear evolution problems by parallelized collocation-interpolation methods. *Comput. Math. Appl.* **34**(12), 71–79 (1997)
7. Carlson, R.E., Foley, T.A.: The parameter R^2 in multiquadric interpolation. *Comput. Math. Appl.* **21**(9), 29–42 (1991)
8. del Castillo-Negrete, D., Carreras, B.A., Lynch, V.E.: Fractional diffusion in plasma turbulence. *Phys. Plasmas* **11**(8), 3854–3864 (2004)
9. Chen, Y.M., Wu, Y.B., Cui, Y.H., Wang, Z.Z., Jin, D.M.: Wavelet method for a class of fractional convection-diffusion equation with variable coefficients. *J. Comput. Sci.* **1**(3), 146–149 (2010)
10. Cheng, A.H.D.: Multiquadric and its shape parameter—A numerical investigation of error estimate, condition number, and round-off error by arbitrary precision computation. *Eng. Anal. Bound. Elem.* **36**(2), 220–239 (2012)
11. Deng, W.H.: Finite element method for the space and time fractional Fokker–Planck equation. *SIAM J. Numer. Anal.* **47**(1), 204–226 (2008)
12. Ding, H.F.: General Padé approximation method for time-space fractional diffusion equation. *J. Comput. Appl. Math.* **299**, 221–228 (2016)
13. Doha, E.H., Bhrawy, A.H., Baleanu, D., Ezz-Eldien, S.S.: The operational matrix formulation of the Jacobi tau approximation for space fractional diffusion equation. *Adv. Differ. Equ.* **2014**(1), 231 (2014)
14. Du, N., Wang, H.: A fast finite element method for space-fractional dispersion equations on bounded domains in R^2 . *SIAM J. Sci. Comput.* **37**(3), A1614–A1635 (2015)
15. Elhay, S., Kautsky, J.: Algorithm 655: IQPACK: FORTRAN subroutines for the weights of interpolatory quadratures. *Acm. T. Math. Softwar.* **13**(4), 399–415 (1987)
16. Ervin, V.J., Roop, J.P.: Variational formulation for the stationary fractional advection dispersion equation. *Numer. Meth. Part. D. E.* **22**(3), 558–576 (2006)
17. Fasshauer, G.E., Zhang, J.G.: On choosing optimal shape parameters for RBF approximation. *Numer. Algor.* **45**(1), 345–368 (2007)
18. Feng, L.B., Zhuang, P., Liu, F., Turner, I., Anh, V., Li, J.: A fast second-order accurate method for a two-sided space-fractional diffusion equation with variable coefficients. *Comput. Math. Appl.* **73**(6), 1155–1171 (2017)

19. Hejazi, H., Moroney, T., Liu, F.W.: Stability and convergence of a finite volume method for the space fractional advection-dispersion equation. *J. Comput. Appl. Math.* **255**, 684–697 (2014)
20. Ichise, M., Nagayanagi, Y., Kojima, T.: An analog simulation of non-integer order transfer functions for analysis of electrode processes. *J. Electroanal. Chem.* **33**(2), 253–265 (1971)
21. Jia, J.H., Wang, H.: A fast finite volume method for conservative space-fractional diffusion equations in convex domains. *J. Comput. Phys.* **310**, 63–84 (2016)
22. Liu, F., Zhuang, P., Turner, I., Anh, V., Burrage, K.: A semi-alternating direction method for a 2-D fractional Fitzhugh–Nagumo monodomain model on an approximate irregular domain. *J. Comput. Phys.* **293**, 252–263 (2015)
23. Liu, Q., Liu, F., Gu, Y.T., Zhuang, P., Chen, J., Turner, I.: A meshless method based on Point Interpolation Method (PIM) for the space fractional diffusion equation. *Appl. Math. Comput.* **256**, 930–938 (2015)
24. Luh, L.T.: The shape parameter in the Gaussian function II. *Eng. Anal. Bound. Elem.* **37**(6), 988–993 (2013)
25. Mainardi, F.: *Fractals and Fractional Calculus Continuum Mechanics*. Springer, Verlag (1997)
26. Meerschaert, M.M., Scheffler, H.P., Tadjeran, C.: Finite difference methods for two-dimensional fractional dispersion equation. *J. Comput. Phys.* **211**(1), 249–261 (2006)
27. Meerschaert, M.M., Tadjeran, C.: Finite difference approximations for two-sided space-fractional partial differential equations. *Appl. Numer. Math.* **56**(1), 80–90 (2006)
28. Nezza, E.D., Palatucci, G., Valdinoci, E.: Hitchhiker’s guide to the fractional Sobolev spaces. *B. Sci. Math.* **136**(5), 521–573 (2012)
29. Nigmatulin, R.: The realization of the generalized transfer equation in a medium with fractal geometry. *Phys. Stat. Sol. B* **133**, 425–430 (1986)
30. Pandey, R.K., Singh, O.P., Baranwal, V.K., Tripathi, M.P.: An analytic solution for the space-time fractional advection-dispersion equation using the optimal homotopy asymptotic method. *Comput. Phys. Commun.* **183**(10), 2098–2106 (2012)
31. Pang, G.F., Chen, W., Sze, K.Y.: Gauss-Jacobi-type quadrature rules for fractional directional integrals. *Comput. Math. Appl.* **66**(5), 597C607 (2013)
32. Podlubny, I.: *Fractional Differential Equations*. Academic Press, San Diego, CA (1999)
33. Qiu, L.L., Deng, W.H., Hesthaven, J.S.: Nodal discontinuous Galerkin methods for fractional diffusion equations on 2D domain with triangular meshes. *J. Comput. Phys.* **298**, 678–694 (2015)
34. Quan, J.R., Chang, C.T.: New insights in solving distributed system equations by the quadrature method-I. *Analysis. Comput. Chem. Eng.* **13**(7), 779–788 (1989)
35. Ray, S.S.: Analytical solution for the space fractional diffusion equation by two-step Adomian Decomposition Method. *Commun. Nonlinear Sci. Numer. Simul.* **14**(4), 1295–1306 (2009)
36. Ray, S.S., Sahoo, S.: Analytical approximate solutions of Riesz fractional diffusion equation and Riesz fractional advection-dispersion equation involving nonlocal space fractional derivatives. *Math. Method. Appl. Sci.* **38**(13), 2840–2849 (2015)
37. Ren, R.F., Li, H.B., Jiang, W., Song, M.Y.: An efficient Chebyshev-tau method for solving the space fractional diffusion equations. *Appl. Math. Comput.* **224**, 259–267 (2013)
38. Rippa, S.: An algorithm for selecting a good value for the parameter c in radial basis function interpolation. *Adv. Comput. Math.* **11**(2), 193–210 (1999)
39. S. Vong, S., Lyu, P., Chen, X., Lei, S.L.: High order finite difference method for time-space fractional differential equations with Caputo and Riemann-Liouville derivatives. *Numer. Algor.* **72**(1), 195–210 (2016)
40. Saadatmandi, A., Dehghan, M.: A tau approach for solution of the space fractional diffusion equation. *Comput. Math. Appl.* **62**(3), 1135–1142 (2011)
41. Sarra, S.A., Sturgill, D.: A random variable shape parameter strategy for radial basis function approximation methods. *Eng. Anal. Bound. Elem.* **33**, 1239–1245 (2009)
42. Shu, C., Richards, B.E.: Application of generalized differential quadrature to solve two-dimensional incompressible Navier-Stokes equations. *Int. J. Numer. Meth. Fluids* **15**(7), 791–798 (1992)

43. Sousa, E.: Numerical approximations for fractional diffusion equations via splines. *Comput. Math. Appl.* **62**(3), 938–944 (2011)
44. Tian, W.Y., Zhou, H., Deng, W.H.: A class of second order difference approximations for solving space fractional diffusion equations. *Math. Comp.* **84**(294), 1703–1727 (2015)
45. Wang, H., Basu, T.S.: A fast finite difference method for two-dimensional space-fractional diffusion equations. *SIAM J. Sci. Comput.* **34**(5), A2444–A2458 (2012)
46. Wu, Y.L., Shu, C.: Development of RBF-DQ method for derivative approximation and its application to simulate natural convection in concentric annuli. *Comput. Mech.* **29**(6), 477–485 (2002)
47. Xu, Q.W., Hesthaven, J.S.: Discontinuous Galerkin method for fractional convection-diffusion equations. *SIAM J. Numer. Anal.* **52**(1), 405–423 (2014)
48. Yang, Z., Yuan, Z., Nie, Y., Wang, J., Zhu, X., Liu, F.: Finite element method for nonlinear Riesz space fractional diffusion equations on irregular domains. *J. Comput. Phys.* **330**, 863–883 (2017)
49. Yıldırım, A., Koçak, H.: Homotopy perturbation method for solving the space-time fractional advection-dispersion equation. *Adv. Water Resour.* **32**(12), 1711–1716 (2009)
50. Yuan, Z.B., Nie, Y.F., Liu, F., Turner, I., Zhang, G.Y., Gu, Y.T.: An advanced numerical modeling for Riesz space fractional advection–dispersion equations by a meshfree approach. *Appl. Math. Model.* **40**(17), 7816–7829 (2016)
51. Zayernouri, M., Karniadakis, G.E.: Fractional spectral collocation methods for linear and nonlinear variable order FPDEs. *J. Comput. Phys.* **293**, 312–338 (2015)
52. Zeng, F.H., Liu, F.W., Li, C.P., Burrage, K., Turner, I., Anh, V.: A Crank–Nicolson ADI spectral method for a two-dimensional Riesz space fractional nonlinear reaction-diffusion equation. *SIAM J. Numer. Anal.* **52**(6), 2599–2622 (2014)
53. Zhu, X.G., Nie, Y.F., Wang, J.G., Yuan, Z.B.: A numerical approach for the Riesz space-fractional Fisher’ equation in two-dimensions. *Int. J. Comput. Math.* **94**(2), 296–315 (2017)